Title

Substratum Compliance Modulates Corneal Fibroblast to Myofibroblast TransformationSubstrate Modulus and Corneal Cell Transformation

Journal

Investigative Ophthalmology & Visual Science, 54(8)

ISSN

0146-0404

Authors

Dreier, Britta
Thomasy, Sara M
Mendonsa, Rima
et al.

Publication Date

2013-08-28

DOI

10.1167/iovs.12-11575

Peer reviewed

Substratum Compliance Modulates Corneal Fibroblast to Myofibroblast Transformation

Britta Dreier,[1] Sara M. Thomasy,[1] Rima Mendonsa,[1] Vijay Krishna Raghunathan,[1] Paul Russell,[1] and Christopher J. Murphy[1,2]

[1]Department of Surgical and Radiological Sciences, School of Veterinary Medicine, University of California, Davis, Davis, California
[2]Department of Ophthalmology and Vision Science, School of Medicine, University of California, Davis, Davis, California

Correspondence: Christopher J. Murphy, Department of Surgical and Radiological Sciences, School of Veterinary Medicine, University of California, Davis, 1220 Tupper Hall, Davis, CA 95616; cjmurphy@ucdavis.edu.

Submitted: December 28, 2012
Accepted: July 9, 2013

Citation: Dreier B, Thomasy SM, Mendonsa R, Raghunathan VK, Russell P, Murphy CJ. Substratum compliance modulates corneal fibroblast to myofibroblast transformation. *Invest Ophthalmol Vis Sci*. 2013;54:5901–5907. DOI:10.1167/iovs.12-11575

Purpose. The transformation of fibroblasts to myofibroblasts is critical to corneal wound healing, stromal haze formation, and scarring. It has recently been demonstrated that the provision of biomimetic substratum topographic cues inhibits the progression toward the myofibroblast phenotype under the influence of transforming growth factor β1 (TGF-β1). The objective of this study was to determine the effect of another fundamental biophysical cue, substrate compliance, on TGF-β1–induced myofibroblast transformation of primary corneal cells isolated from human and rabbit corneas.

Methods. Human and rabbit corneal fibroblasts were cultured on surfaces of varying substrate compliance (4–71 kPa) and tissue culture plastic (TCP) (>1 gigapascal [GPa]). Cells were cultured in media containing TGF-β1 at concentrations of 0, 1, or 10 ng/mL for 72 hours. RNA and protein were collected from cells cultured on polyacrylamide gels and TCP and were analyzed for the expression of α-smooth muscle actin (α-SMA), a key marker of myofibroblast transformation, using quantitative PCR, immunocytochemistry, and Western blot.

Results. Cells grown on more compliant substrates demonstrated significantly reduced amounts of α-SMA mRNA compared with TCP. Immunocytochemistry and Western blot analysis determining the presence of α-SMA corroborated this finding, thus confirming a reduced transformation to the myofibroblast phenotype on more compliant substrates compared with cells on TCP in the presence of TGF-β1.

Conclusions. These data indicate that substrate compliance modulates TGF-β1–induced expression of α-SMA and thus influences myofibroblast transformation in the corneal stroma. This provides further evidence that biomimetic biophysical cues inhibit myofibroblast transformation and participate in stabilizing the native cellular phenotype.

Keywords: myofibroblast transformation, biophysical cues, α-smooth muscle actin, corneal wound healing

Upon wounding of the corneal stroma, the quiescent stromal keratocytes differentiate into more proliferative and metabolically active fibroblasts and subsequently myofibroblasts, a transition termed the *keratocyte-fibroblast-myofibroblast* (KFM) *transformation*.[1–3] While the transformation of fibroblasts to myofibroblasts is crucial for normal wound healing, excessive numbers of myofibroblasts and/or their prolonged persistence are associated with corneal scarring and compromised vision.[4–6] Specifically, the presence of myofibroblasts within the remodeling corneal wound results in increased light scatter, decreased corneal crystallin expression, and disorganized extracellular matrix production, all of which can contribute to stromal haze.[7] Fibroblasts have also been implicated as a source of stromal haze, reduced corneal crystallin, and altered extracellular matrix expression.[5] Thus, understanding the biochemical mediators and biophysical cues that modulate the KFM pathway is critical for the development of novel therapeutic strategies to decrease corneal scarring.

Corneal stromal cells in vivo are exposed to soluble biochemical signals, as well as biophysical cues from their native microenvironment. The corneal stroma is composed of sheet-like fibrillar parallel bundles of collagen with a sparse population of keratocytes located between the lamellae. It has been previously demonstrated that substratum topography can modulate fundamental behaviors, including cell shape regulation and migration in primary rabbit keratocytes, fibroblasts, and myofibroblasts.[2] In addition, it has been reported that the provision of topographic cues inhibits the transformation of corneal stromal cells to myofibroblasts.[8] Thus, we hypothesized that another ubiquitous biophysical cue, substratum compliance (the inverse of stiffness), may also modulate the transition of corneal stromal cells to myofibroblasts. The elastic modulus, a measure of compliance, of the different layers of the human cornea has recently been described.[9] We used these data to guide the fabrication of model substrates possessing values for compliance in the biomimetic range for the corneal stroma.

Primary corneal keratocytes transition to activated fibroblasts in vitro when cultured in serum-containing medium.[10] The transformation of fibroblasts to myofibroblasts can then be induced in vitro by the addition of transforming growth factor β1 (TGF-β1) to the growth medium.[10] Myofibroblasts are frequently identified by their expression of α-smooth muscle actin (α-SMA) fibers.[10] The objective of this study was to determine the effect of substratum compliance on the TGF-β1–induced transi-

tion of corneal fibroblasts to myofibroblasts through evaluation of α-SMA mRNA and protein expression.

Methods

Fabrication of Compliant Polyacrylamide Substrates

Polyacrylamide hydrogels with an elastic modulus of 4, 28, 52, and 71 kPa, shown to be suitable for cell culture, were fabricated as previously described.[11] To remove unreacted reagents, the gels were rinsed three times in PBS (HyClone; Fisher Scientific, Waltham, MA) and were sterilized in a hydrated state by exposure to short-wavelength UV light (280 nm) for 20 minutes. Following another PBS rinse, the gels were stored in a 5% CO_2 incubator at 37°C for at least 48 hours to attain full hydration, followed by three additional PBS rinses. The gels were then allowed to equilibrate in growth medium for 24 hours. Atomic force microscopy (AFM) was used to validate the elastic modulus of the fully hydrated gels, and the mean ± SD elastic moduli of the gels used were 4 ± 2, 28 ± 4, 52 ± 7, and 71 ± 5 kPa.[11,12] The 4-kPa hydrogel was used to mimic the normal rabbit stroma,[13] and the 28-kPa hydrogel was used to mimic the normal human stroma.[9] Standard tissue culture plastic (stiffness of >1 gigapascal [GPa]) was used as a control.

Isolation and Culture of Primary Stromal cells From Human Corneas

Primary human corneal fibroblasts (HCFs) were isolated from donated human corneoscleral rims not suitable for transplant (Heartland Lions Eye Bank, Kansas City, MO). All experiments complied with the Declaration of Helsinki. The cell isolation was performed as previously described[14] with slight modifications. Briefly, the sclera and limbal regions were removed, and the remaining tissue was immersed in dispase solution (1.2 U/mL; Boehringer, Mannheim, Germany) at 37°C for 4 hours. Corneal epithelial and endothelial cells were removed by gentle debridement of the anterior and posterior surface. The remaining corneal stroma containing the keratocytes was incubated in four-well plates (Nunc, Penfield, NY) containing Dulbecco's modified Eagle's medium (DMEM) high glucose (Life Technologies, Carlsbad, CA) supplemented with 10% fetal bovine serum (FBS) (Atlanta Biologicals, Lawrenceville, GA) and 1% penicillin-streptomycin-amphotericin B (P/S/F, Life Technologies). The presence of serum is known to cause a transition of quiescent keratocytes to the more metabolically active fibroblast phenotype.[15,16] Fibroblasts were allowed to migrate from the corneal tissue and expand over a period of several weeks. Human corneal fibroblasts from up to six different donors were pooled and cultured in DMEM high glucose supplemented with 10% FBS and 1% P/S/F at 37°C under 5% CO_2 and were utilized between passages two and seven. To determine the lowest TGF-β1 concentration required to induce maximal α-SMA expression in HCFs, we initially treated HCFs grown on tissue culture plastic (TCP) with a range of TGF-β1 concentrations (0, 0.25, 0.5, 1, 2.5, 5, 7.5, or 10 ng/mL) for 72 hours in medium containing 10% FBS. In all subsequent experiments, the transformation of HCFs to myofibroblasts was induced by exposure to 1 or 10 ng/mL of TGF-β1 (T7039; Sigma-Aldrich Corp., St. Louis, MO) for 72 hours in medium containing 10% FBS.

Isolation and Culture of Primary Stromal Cells From Rabbit Corneas

Primary keratocytes were isolated as previously described[8] from freshly enucleated young rabbit eyes (Pel-Freez, Rogers, AR), which were examined before dissection and processed within 36 hours of tissue harvest. Cells were cultured in DMEM low glucose supplemented with 10% FBS and 1% P/S/F. Cells were incubated for 3 days to assure transition to the fibroblast phenotype. A TGF-β1 dose-response concentration for induction of rabbit corneal fibroblasts (RCFs) to myofibroblasts on TCP was previously determined in our laboratory.[8] In the present study, the cells were exposed for 72 hours to 1 or 10 ng/mL of TGF-β1 in medium containing 10% FBS to induce the transformation of RCFs to myofibroblasts.

Cell Culture on Compliant Polyacrylamide Substrates

Before cell plating, gels were treated for 5 minutes with a mixture of 97% collagen I and 3% collagen III (PureCol; Advanced Biomatrix, Fremont, CA) diluted in an equal volume of 12 mM HCl (Acros Organics, Geel, Belgium) to achieve a molecular coating of collagen and were subsequently rinsed twice with serum-free DMEM. The compliance of the gels was unaltered when coated with collagen as determined by AFM (data not shown). Fibroblasts were plated in six-well dishes at a density of 5×10^4 to 2×10^5 per well (5×10^4 on TCP, 2×10^5 on 4-kPa gels, and 1×10^5 on 28-, 52-, or 71-kPa gels) in DMEM low glucose (RCFs) or DMEM high glucose (HCFs) containing 1% P/S/F and 10% FBS and were left to adhere overnight. A higher cell density was used on gels because cells showed a lower proliferation rate on more compliant substrates, as well as to ensure that an adequate amount of mRNA or protein could be collected from the gels.[17] The following day, the cells were inspected by light microscopy to ensure a comparable cell density on all substrates, and the medium was exchanged with the appropriate medium for each cell type containing 10% FBS, 1% P/S/F, and 0, 1, or 10 ng/mL of TGF-β1. After 72 hours, cells were harvested for RNA, fixation, or protein isolation.

RNA Extraction and Quantitative Real-time PCR

RNA was extracted 72 hours after TGF-β1 induction using the RNeasy kit (Qiagen, Valencia, CA) following the manufacturer's protocol. Quantitative real-time PCR (qPCR) was performed with 50 ng of RNA per sample using the Taqman One-Step PCR kit (Life Technologies) and aptamers specific to human and rabbit α-SMA (*ACTA2*, Hs00426835_g1 or Oc03399251_m1; Life Technologies) in total volumes of 10 μL per reaction. The reverse transcription reaction was performed in a StepOne qPCR machine (Life Technologies) for 30 minutes at 50°C, followed by PCR enzyme activation for 10 minutes at 95°C and 40 cycles of 60°C for 1 minute, followed by 95°C for 15 seconds. Glyceraldehyde 3-phosphate dehydrogenase (*GAPDH*, Hs99999905_m1 or Oc03823402_g1) served as a reference. The reactions were run in triplicate, and each experiment was performed at least three times. Unless stated otherwise, gene expression was normalized relative to the expression of mRNA from cells grown on TCP with 10 ng/mL of TGF-β1 added to the medium, which was given an arbitrary value of 1.0.

Protein Sample Preparation

After induction for 72 hours in 10 ng/mL of TGF-β1–containing medium, cells were lysed on ice with radioimmunoprecipitation assay (RIPA) buffer containing Halt Protease Inhibitor Cocktail (Thermo Fisher Scientific, Rockford, IL). Insoluble cellular debris was removed by centrifugation at 14,000*g* in a cooled tabletop microcentrifuge for 5 minutes. The protein concentration was determined using a modified Lowry assay (DC Protein Assay; Bio-Rad, Hercules, CA) with bovine serum albumin as the standard. The samples were prepared for electrophoresis by incubation with 5× Laemmli buffer at 95°C for 5 minutes.

Investigative Ophthalmology & Visual Science

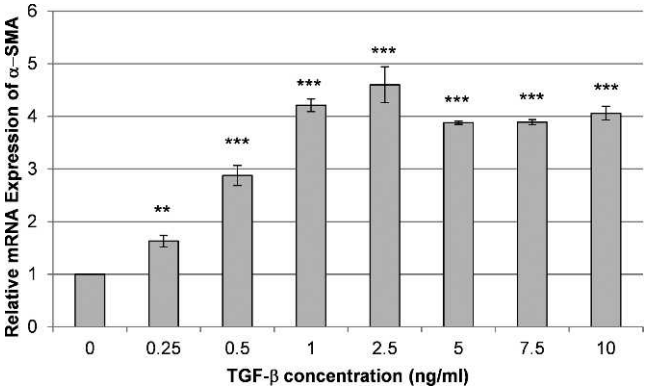

FIGURE 1. Transforming growth factor β1 induces the expression of α-SMA in HCFs. Shown is a representative graph from one of at least three experiments demonstrating the relative mRNA expression of α-SMA in HCFs cultured on TCP for 72 hours with various concentrations of TGF-β1 and 10% serum added to the medium. Maximal expression of α-SMA was achieved at 1 ng/mL of TGF-β. Data are mean ± SD. *Asterisks* indicate statistically significant differences compared with the expression in cells cultured without added TGF-β1 (***$P < 0.001$ and **$P < 0.01$, one-way ANOVA, followed by Holm-Sidak pairwise comparison test).

Western Blot Analysis

Equivalent amounts of protein (10 μg) were loaded onto a 10% NuPAGE Bis-Tris Pre-Cast gel (Life Technologies). Gel electrophoresis was performed at 140 V for 1 hour, followed by transfer to a nitrocellulose membrane (Life Technologies) at 200 milliampere for 2 hours. Successful protein transfer was confirmed by Ponceau S staining. The membrane was blocked for 1 hour at room temperature (RT) with SuperBlock blocking buffer (Thermo Fisher Scientific), followed by incubation with the primary antibody mouse anti–α-SMA (Sigma-Aldrich Corp.) diluted 1:20,000 in 10% SuperBlock in PBS overnight at 4°C. The blot was washed three times in PBS with 0.1% Tween-20 (PBS-T) before incubating with peroxidase-conjugated goat anti-mouse antibody (KPL, Gaithersburg, MD) diluted 1:20,000 for 1 hour at RT. After washing three times with PBS-T and once with PBS, protein bands of interest were detected using an enhanced chemiluminescent Western blot reagent (ECL plus, GE Healthcare, Pittsburgh, PA) and an ImageQuant 350 charge-coupled device camera (GE Healthcare). Afterward, the same blots were used for detection of GAPDH (mouse anti-GAPDH, catalog number MAB374; EMT Millipore, Billerica, MA) as a reference protein. Densitometry analyses were done with ImageJ software (National Institutes of Health, Bethesda, MD).[18] Western blot analysis was performed on samples from five independent experiments.

Immunocytochemistry and Fluorescent Microscopy

Rabbit corneal fibroblasts plated on compliant substrates and TCP were treated with 10 ng/mL of TGF-β1 as described and fixed for 20 minutes at RT with 4% formaldehyde (Polysciences Inc., Warrington, PA) in PBS and subsequently incubated with 0.3% (v/v) H_2O_2 (Sigma-Aldrich Corp.) in ice-cold PBS for 30 minutes. Nonspecific binding sites were blocked with blocking solution (10% [v/v] FBS/10% [v/v] SuperBlock in PBS) for 1 hour at RT. Cells were incubated with the primary antibody (mouse anti–α-SMA, catalog number A5228; Sigma-Aldrich Corp.) 1:100 in blocking solution for 1 hour at 37°C and washed three times in PBS. Incubation with secondary antibody (goat anti-mouse IgG, AlexaFluor 488; Life Technologies) 1:250 in blocking solution for 30 minutes at 37°C was followed by three washes in PBS. F-actin was stained with AlexaFluor 568 phalloidin (Life Technologies) 1:250 in blocking solution for 30 minutes at RT. After three PBS washes, nuclei were stained for 5 minutes at RT with 4′,6-diamidino-2-phenylindole (BioGenex, San Ramon, CA) 1:7500 in PBS. Cells were imaged in PBS with an ×10 objective using the Axiovert 200 M microscope (Carl Zeiss, Jena, Germany).

Statistical Analysis

Statistical analyses were performed using Sigma Plot 11 (Systat Software, Inc., San Jose, CA). Within one experiment, all data sets were compared with one-way ANOVA or two-way ANOVA as indicated. When variability between the data set means was determined to be significant, a Holm-Sidak pairwise comparison test was used to compare these data sets. The level for statistical significance was set at $P < 0.05$ for all comparisons. Within the figures, statistically significant differences are denoted with *$P < 0.05$, **$P < 0.01$, or ***$P < 0.001$ unless stated otherwise.

RESULTS

We first determined the TGF-β1 concentration that would induce complete transformation of HCFs to myofibroblasts under our conditions by testing a range of TGF-β1 concentrations. The addition of TGF-β1 to the culture medium for 72 hours stimulated the expression of the myofibroblast marker α-SMA in HCFs as previously described.[16] The mRNA expression of α-SMA showed a clear dose response to TGF-β1 at concentrations from 0 to 1 ng/mL, while concentrations from 1 to 10 ng/mL did not cause a further increase on TCP (Fig. 1).

In HCFs grown in serum-containing medium, α-SMA mRNA expression was decreased on the most compliant substrates (4, 28, and 52 kPa) compared with TCP (Fig. 2). However, without added TGF-β1, these differences were not statistically significant. As anticipated, treatment with 1 or 10 ng/mL of TGF-β1 significantly increased the mRNA expression of α-SMA on TCP compared with HCFs cultured without TGF-β1 ($P < 0.001$). Notably, increased α-SMA expression following TGF-β1 treatment was markedly less pronounced in HCFs on compliant substrates (Fig. 2). At concentrations of 1 and 10 ng/mL of TGF-β1, HCFs on all gels showed less α-SMA mRNA expression compared with cells grown on TCP. Cells on the 4-kPa substrates showed a further reduced expression compared with cells grown on less compliant hydrogels at both TGF-β1 concentrations.

As expected, treatment with TGF-β1 also induced the expression of α-SMA mRNA in RCFs cultured on TCP (Fig. 3); consistent with our findings in HCFs, RCFs exhibited a reduced mRNA expression of α-SMA in response to TGF-β1 on each compliance compared with TCP (***$P < 0.001$). Rabbit corneal fibroblasts on 4-kPa gels expressed significantly less α-SMA mRNA than cells on any of the other hydrogels when treated with TGF-β1. Without TGF-β1 treatment, the expression in cells on 4-kPa gels was significantly lower compared with cells on the 52-kPa gels but not compared with cells on the 28-kDa or 71-kDa gels. Notably, even without the addition of TGF-β1, α-SMA mRNA expression was reduced in RCFs grown on all of the tested compliant substrates compared with those grown on TCP ($P < 0.001$).

To confirm this observation, RCFs cultured in the absence or presence of 10 ng/mL of TGF-β1 on substrates with varying compliances were stained for the expression of F-actin and α-SMA (Fig. 4). Substrates of low (TCP), moderate (28 kPa), and high (4 kPa) compliance were chosen because these showed the most dramatic differences in α-SMA expression. As expected, the majority of cells cultured on TCP showed strong α-SMA staining (green) when treated with TGF-β1, thus

Investigative Ophthalmology & Visual Science

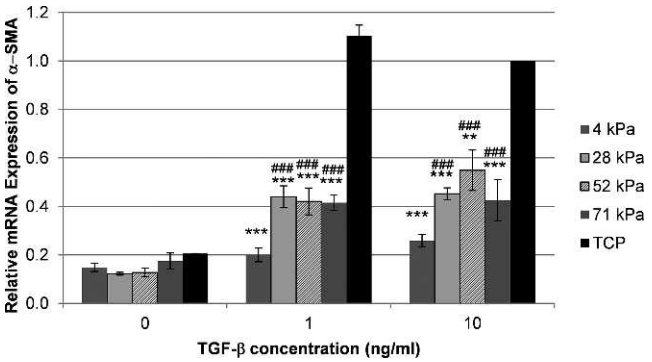

Figure 2. Substratum compliance restricts TGF-β1–induced expression of α-SMA in HCFs. Shown is a representative graph from one of at least three independent experiments demonstrating the average amounts of relative α-SMA mRNA expression in HCFs grown on gels and TCP cultured with 0, 1, or 10 ng/mL of TGF-β1 as determined by qPCR. The addition of TGF-β1 induced an increased α-SMA expression on all substrates. Following treatment with 1 or 10 ng/mL of TGF-β1, HCFs grown on very stiff substrate (TCP) had markedly more α-SMA expression compared with cells grown on more compliant substrates. In the presence of 1 or 10 ng/mL of TGF-β1, the lowest α-SMA expression was measured in HCFs grown on 4-kPa gels. Treatment with 1 or 10 ng/mL of TGF-β1 significantly increased α-SMA mRNA expression ($P < 0.001$) on TCP compared with culture without TGF-β1. The expression of α-SMA in HCFs on TCP treated with 10 ng/mL of TGF-β1 was arbitrarily set as 1.0. Data are mean ± SD. Indicated are statistically significant differences in α-SMA expression between cells grown on compliant substrates and TCP for each TGF-β1 concentration (***$P < 0.001$ and **$P < 0.01$) and between cells grown on 4-kPa gels and less compliant gels (###$P < 0.001$) (two-way ANOVA, followed by Holm-Sidak pairwise comparison test).

confirming the myofibroblast phenotype. In contrast, even in the presence of TGF-β1, only a few cells (28-kPa gels) or no cells (4-kPa gels) stained positive for α-SMA but showed a clear F-actin staining, although the incidence of stress fibers was greatest in cells cultured on TCP compared with more compliant substrates.

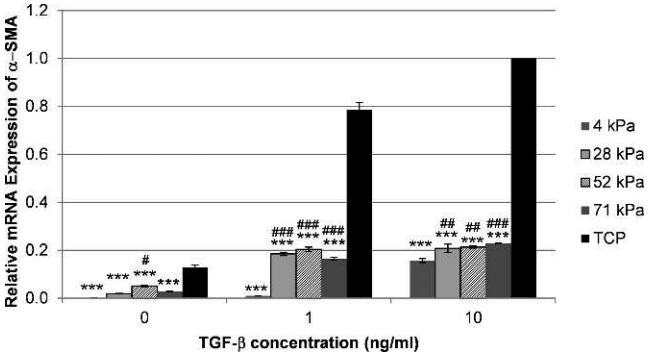

Figure 3. Substratum compliance modulates α-SMA mRNA expression in RCFs. Treatment with 1 or 10 ng/mL of TGF-β1 significantly increased α-SMA mRNA expression ($P < 0.001$) on TCP compared with culture without TGF-β1. Following treatment with TGF-β1, cells on the most compliant substrate (4 kPa), mimicking the normal rabbit stroma, expressed significantly reduced amounts of α-SMA mRNA compared with any other substrate. Shown is a representative graph from one of three independent experiments. The expression of α-SMA in RCFs on TCP treated with 10 ng/mL of TGF-β1 was arbitrarily set as 1.0. Data are mean ± SD. Indicated are statistically significant differences in the α-SMA expression between cells grown on compliant substrates and TCP for each TGF-β1 concentration (***$P < 0.001$) and between cells grown on 4-kPa gels and less compliant gels (###$P < 0.001$, ##$P < 0.01$, and #$P < 0.05$) (two-way ANOVA, followed by Holm-Sidak pairwise comparison test).

To determine if protein expression was consistent with the previous immunocytochemistry and mRNA results, Western blot analyses were performed using cell lysates of RCFs grown on substrates of different compliances and treated with 10 ng/mL of TGF-β1. A TGF-β1 concentration of 10 ng/mL was chosen for this experiment because we wanted to expose the cells to a signaling environment that would ensure myofibroblast transformation. As anticipated, we detected significantly reduced amounts of α-SMA protein in RCFs cultured on more compliant substrates compared with RCFs grown on TCP (Fig. 5). Protein expression of α-SMA appears to be graded, with cells on more compliant hydrogels exhibiting lower expression than cells on less compliant gels. However, these differences between the gels were not statistically significant; in contrast to the qPCR data, no significant differences were observed between the α-SMA protein expression in cells on 4-kPa gels and cells on any other gel. Thus, compared with the impact of substrate compliance on mRNA expression, the differences in protein expression were less pronounced.

Discussion

Corneal cells in vivo are exposed to biophysical cues intrinsic to the extracellular matrix, including topography and compliance.[9,19,20] Increasing numbers of publications from our laboratory and others have documented several cell types to be highly influenced by biophysical cues resulting in changes in their cellular behavior, including cell shape, proliferation, adhesion, and migration, as well as gene expression.[11,17,21–24] Previous studies[8,25] from our laboratory detailed the impact of substratum topographic cues on the transition of corneal fibroblasts to myofibroblasts. We have recently profiled the elastic moduli of human corneal stromal elements[9] informing the subsequent design and fabrication of substrates possessing biologically relevant values for substratum compliance. The mean ± SD elastic modulus of the anterior stroma of the human cornea was measured using AFM as 33.1 ± 6.1 kPa[9]; thus, the 28-kPa gels used in the present study approximated the compliance of the native human corneal stroma. The 4-kPa gels most closely mimic the rabbit corneal stroma, which is markedly more compliant than the human corneal stroma, with a mean ± SD elastic modulus of 1.1 ± 0.58 kPa as reported by Thomasy et al.[13] It should be noted that other research groups have documented notably different values for the compliance of the corneal stroma. For instance, Winkler et al.[26] measured elastic moduli ranging from 892 to 1861 Pa for the anterior cornea, while Lombardo et al.[27] reported values ranging from 1.14 to 2.63 megapascal. As previously detailed,[9,28] several factors likely account for these differences, including sample preparation, the specific location within the corneal tissue (e.g., anterior versus posterior stroma), and, most importantly, differences in the techniques used for determining the compliance values. For a more detailed presentation of the differences in techniques utilized to obtain elastic modulus values in tissues, we refer the reader to a review article by McKee et al.[28] In the present study, the compliance measurements were internally consistent in that the same technique, AFM, was used to determine the elastic modulus of the cornea[9,13] and of the compliant substrates.[11,12]

The transformation of rabbit corneal keratocytes and fibroblasts to myofibroblasts has been the subject of several studies[8,16,25,29,30]; however, the myofibroblast transformation of human corneal cells in vitro has rarely been investigated, most likely because of the limited availability of suitable tissue. An important study by Jester et al.[31] described the TGF-β1–induced transformation of primary human corneal keratocytes and immortalized corneal fibroblasts to myofibroblasts in vitro. To determine the optimal TGF-β1 concentration required to induce

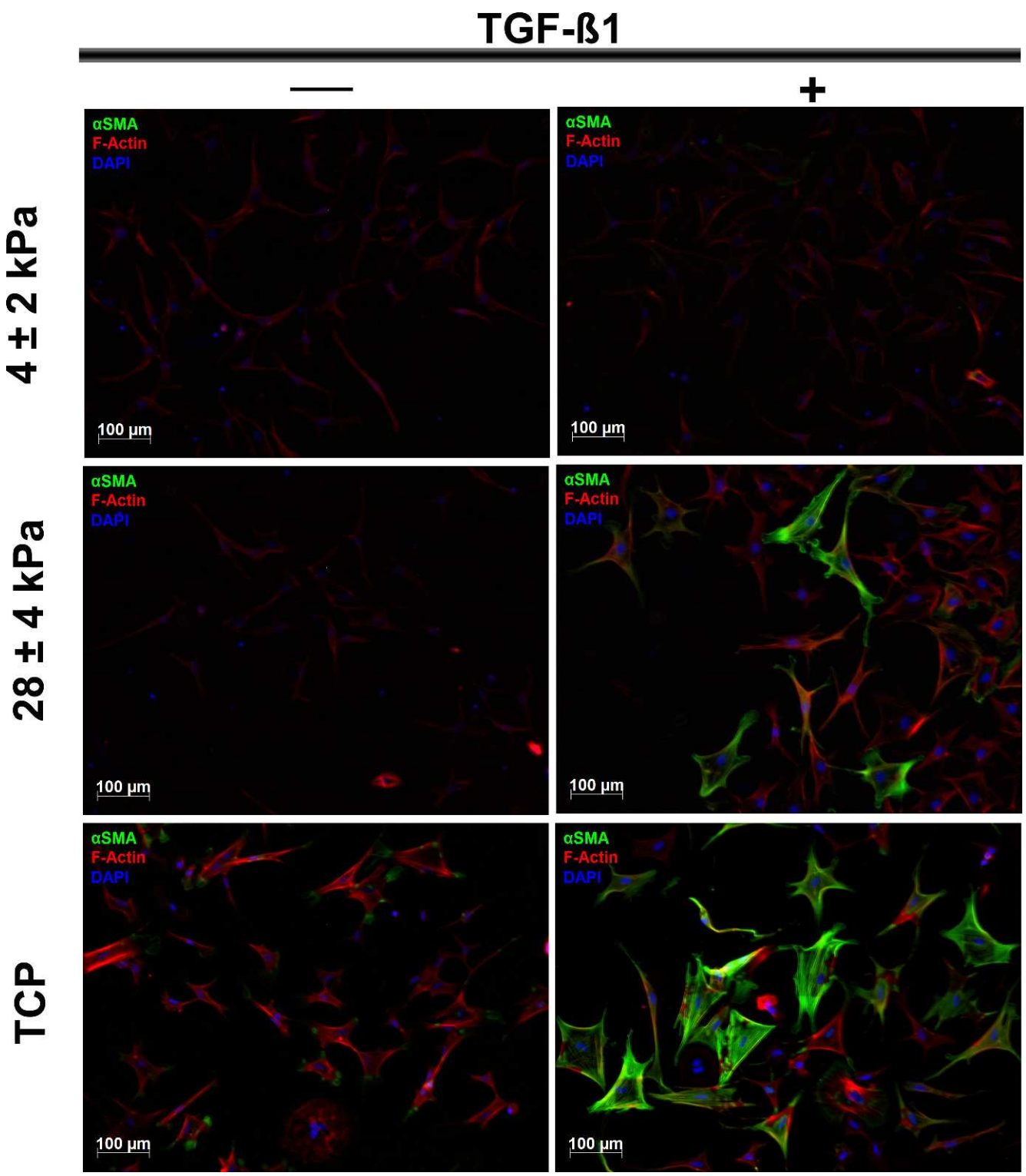

Figure 4. Substratum compliance limits the transformation to the myofibroblast phenotype. Representative images show the fluorescent staining of α-SMA (*green*), F-actin (*red*), and 4′,6-diamidino-2-phenylindole (DAPI; *blue*) in RCFs cultured in the absence or presence of 10 ng/mL of TGF-β1 on substrates with varying compliance. The majority of cells on TCP displayed strong staining for α-SMA when exposed to TGF-β1, thus confirming the myofibroblast phenotype in these cells. In contrast, few cells (on 28-kPa gels) or no cells (on 4-kPa gels) stained positive for α-SMA, even in the presence of 10 ng/mL of TGF-β1. All cells show clear staining of F-actin, although the incidence of stress fibers was greatest in cells on TCP. *Scale bar*: 100 µm; ×10 objective.

Investigative Ophthalmology & Visual Science

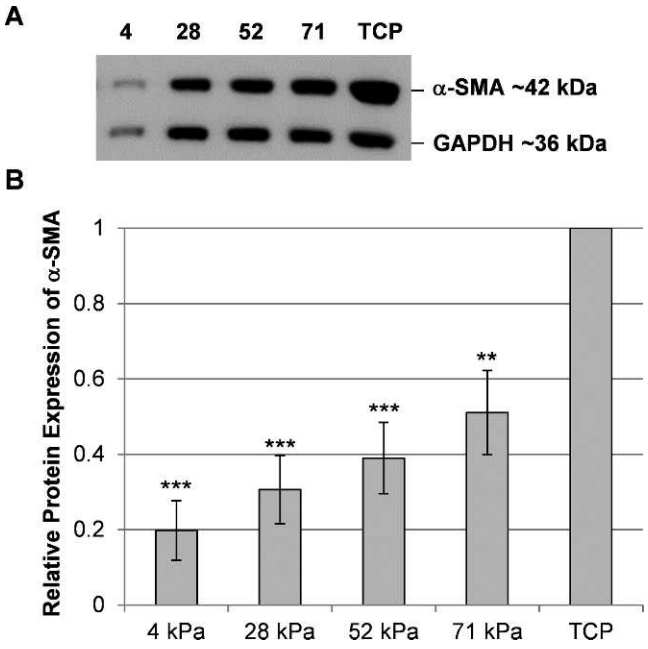

Figure 5. Substratum compliance modulates α-SMA protein expression in RCFs. A representative Western blot from one experiment demonstrates the reduced expression of α-SMA protein in RCFs cultured for 72 hours with 10 ng/mL of TGF-β1 on more compliant substrates compared with TCP. (**A**) As a loading control, GAPDH was detected as a 36-kDa band, while α-SMA was detected as a 42-kDa band. (**B**) A densitometry analysis was performed to account for differences in the loaded protein amounts. The graph shows mean ± SEM values obtained from five independent experiments. *Asterisks* indicate statistically significant differences in the α-SMA protein expression between cells on compliant substrates and TCP (***$P < 0.001$ and **$P < 0.01$, one-way ANOVA, followed by Holm-Sidak pairwise comparison test). The differences in the α-SMA expression in cells on the different gels were not statistically different from each other.

the transformation of primary HCFs to myofibroblasts, we tested a range of TGF-β1 concentrations. In the present study, 1 ng/mL of TGF-β1 in serum-containing medium was sufficient to induce maximal expression of α-SMA in HCFs grown on TCP. Because preliminary investigations showed that compliance inhibits the transformation to the myofibroblast phenotype,[32] a concentration of 10 ng/mL of TGF-β1 was also included in all subsequent experiments to provide TGF-β1 in excess of the empirically determined concentration for maximal transformation.

We observed reduced α-SMA mRNA expression for HCFs and reduced α-SMA mRNA and protein expression for RCFs on substrates mimicking the compliance of the normal human and rabbit stroma, respectively. The strongest effect was observed in TGF-β1–treated cells grown on the most compliant substrate (4 kPa), which showed further reduced α-SMA mRNA expression compared with cells on any of the less compliant hydrogels. Our data provide evidence that the rabbit, a predominant animal model in vision research, is a valid model to study the impact of changes in local compliance on myofibroblast biology. Notably, the magnitude of the effect of compliance differed in both species such that RCFs appeared to be more strongly modulated by changes in compliance compared with HCFs, even without the addition of TGF-β1. These differences in the cellular responsiveness to changes in compliance are likely due to the specific in vivo microenvironments of the rabbit and human corneal stroma, which most notably differ in their intrinsic compliances.[9,13] Another factor that might contribute to the observed differences between human and rabbit corneal cells is the difference in age of the donor tissues because it was not possible to age match the tissues from the two species. Tissues were obtained from young rabbits in good health, whereas human corneal specimens were from donors of variable age (and generally older) individuals.

Similar to the observations made in the present study, a recent *Investigative Ophthalmology & Visual Science* publication reported an increased TGF-β–induced transformation of rabbit corneal keratocytes to a myofibroblast phenotype when cultured on less compliant substrates such as collagen-coated dishes and compressed collagen matrices compared with more compliant uncompressed collagen matrices.[33] In addition, it has previously been reported that substratum compliance restricts the transformation of fibroblasts into myofibroblasts in human gingival fibroblasts,[34] lung fibroblasts,[35] and valvular interstitial cells,[36] as shown by a decreased TGF-β1–induced expression of α-SMA. Our data with corneal fibroblasts are consistent with these previous reports and highlight the potential impact of stromal compliance on wound healing processes in the cornea.

In other tissues, fibrosis increases the elastic modulus.[37–39] Similarly, the corneal tissue may undergo alterations in compliance throughout the stromal wound healing process, although further work is necessary to establish the precise effect of corneal wounding on the biomechanics of the cornea. It is possible that alterations in corneal compliance throughout wound healing, as well as with aging, disease states, and therapeutic interventions (e.g., cross-linking), will affect the genesis and eventual disappearance of myofibroblasts from the corneal stromal wound bed. The use of substrates in vitro that mimic the compliance of healthy corneas and corneas undergoing wound healing may more accurately predict the outcome of wound healing processes in vivo. Additionally, therapeutic strategies aimed at modulating the compliance of the wound bed microenvironment may inhibit the genesis and promote the clearance of myofibroblasts from the wound bed during healing.

In conclusion, our data document substratum compliance to modulate the expression of α-SMA in human and rabbit corneal stromal cells in vitro, with more compliant substrates inhibiting the transition of fibroblasts to myofibroblasts. Corneal diseases, therapeutic interventions such as cross-linking that decrease compliance, and possibly stromal wound healing processes may increase the modulus of the corneal stroma, which likely promotes the transformation of fibroblasts to myofibroblasts in vivo. The demonstrated relevance of substratum compliance in fibroblast to myofibroblast transformation suggests that biologically relevant biophysical cues should be incorporated in in vitro studies, as well as inform the design and fabrication of improved keratoprosthetics.

Acknowledgments

The authors thank Kunal Patel, Jasmyne Sermeno, and Brad Rose for technical assistance.

Supported by National Institutes of Health Grants R01EY016134, R01EY019970, K08EY021142, and P30EY12576 and by an unrestricted grant from Research to Prevent Blindness.

Disclosure: **B. Dreier**, None; **S.M. Thomasy**, None; **R. Mendonsa**, None; **V.K. Raghunathan**, None; **P. Russell**, None; **C.J. Murphy**, None

References

1. Snyder MC, Bergmanson JP, Doughty MJ. Keratocytes: no more the quiet cells. *J Am Optom Assoc*. 1998;69:180–187.
2. Jester JV, Petroll WM, Barry PA, Cavanagh HD. Expression of α-smooth muscle (α-SM) actin during corneal stromal wound healing. *Invest Ophthalmol Vis Sci*. 1995;36:809–819.
3. Netto MV, Mohan RR, Ambrosio R Jr, Hutcheon AE, Zieske JD, Wilson SE. Wound healing in the cornea: a review of refractive

surgery complications and new prospects for therapy. *Cornea*. 2005;24:509–522.

4. Saika S, Yamanaka O, Sumioka T, et al. Fibrotic disorders in the eye: targets of gene therapy. *Prog Retin Eye Res*. 2008;27:177–196.
5. Jester JV, Moller-Pedersen T, Huang J, et al. The cellular basis of corneal transparency: evidence for 'corneal crystallins'. *J Cell Sci*. 1999;112(pt 5):613–622.
6. Myrna KE, Pot SA, Murphy CJ. Meet the corneal myofibroblast: the role of myofibroblast transformation in corneal wound healing and pathology. *Vet Ophthalmol*. 2009;12(suppl 1):25–27.
7. Jester JV, Budge A, Fisher S, Huang J. Corneal keratocytes: phenotypic and species differences in abundant protein expression and in vitro light-scattering. *Invest Ophthalmol Vis Sci*. 2005;46:2369–2378.
8. Myrna KE, Mendonsa R, Russell P, et al. Substratum topography modulates corneal fibroblast to myofibroblast transformation. *Invest Ophthalmol Vis Sci*. 2012;53:811–816.
9. Last JA, Thomasy SM, Croasdale CR, Russell P, Murphy CJ. Compliance profile of the human cornea as measured by atomic force microscopy. *Micron*. 2012;43:1293–1298.
10. Jester JV, Barry-Lane PA, Cavanagh HD, Petroll WM. Induction of α-smooth muscle actin expression and myofibroblast transformation in cultured corneal keratocytes. *Cornea*. 1996;15:505–516.
11. Wood JA, Shah NM, McKee CT, et al. The role of substratum compliance of hydrogels on vascular endothelial cell behavior. *Biomaterials*. 2011;32:5056–5064.
12. Thomasy SM, Wood JA, Kass PH, Murphy CJ, Russell P. Substratum stiffness and latrunculin B regulate matrix gene and protein expression in human trabecular meshwork cells. *Invest Ophthalmol Vis Sci*. 2012;53:952–958.
13. Thomasy SM, McKee CT, Sadeli AR, et al. Elastic modulus of the rabbit cornea as measured by atomic force microscopy: epithelium to endothelium. In: Abstracts: 43rd Annual Meeting of the American College of Veterinary Ophthalmologists, Portland, Oregon, USA, October 17–20, 2012. *Vet Ophthalmol*. 2013;16:E1–E21.
14. Liliensiek SJ, Campbell S, Nealey PF, Murphy CJ. The scale of substratum topographic features modulates proliferation of corneal epithelial cells and corneal fibroblasts. *J Biomed Mater Res A*. 2006;79:185–192.
15. Masur SK, Dewal HS, Dinh TT, Erenburg I, Petridou S. Myofibroblasts differentiate from fibroblasts when plated at low density. *Proc Natl Acad Sci U S A*. 1996;93:4219–4223.
16. Jester JV, Ho-Chang J. Modulation of cultured corneal keratocyte phenotype by growth factors/cytokines control in vitro contractility and extracellular matrix contraction. *Exp Eye Res*. 2003;77:581–592.
17. Wood JA, McKee CT, Thomasy SM, et al. Substratum compliance regulates human trabecular meshwork cell behaviors and response to latrunculin B. *Invest Ophthalmol Vis Sci*. 2011;52:9298–9303.
18. Schneider CA, Rasband WS, Eliceiri KW. NIH Image to ImageJ: 25 years of image analysis. *Nat Methods*. 2012;9:671–675.
19. Abrams GA, Goodman SL, Nealey PF, Franco M, Murphy CJ. Nanoscale topography of the basement membrane underlying the corneal epithelium of the rhesus macaque. *Cell Tissue Res*. 2000;299:39–46.
20. Last JA, Liliensiek SJ, Nealey PF, Murphy CJ. Determining the mechanical properties of human corneal basement membranes with atomic force microscopy. *J Struct Biol*. 2009;167:19–24.
21. Diehl KA, Foley JD, Nealey PF, Murphy CJ. Nanoscale topography modulates corneal epithelial cell migration. *J Biomed Mater Res A*. 2005;75:603–611.
22. Karuri NW, Porri TJ, Albrecht RM, Murphy CJ, Nealey PF. Nano- and microscale holes modulate cell-substrate adhesion, cytoskeletal organization, and –beta1 integrin localization in SV40 human corneal epithelial cells. *IEEE Trans Nanobioscience*. 2006;5:273–280.
23. Liliensiek SJ, Wood JA, Yong J, Auerbach R, Nealey PF, Murphy CJ. Modulation of human vascular endothelial cell behaviors by nanotopographic cues. *Biomaterials*. 2010;31:5418–5426.
24. Teixeira AI, Nealey PF, Murphy CJ. Responses of human keratocytes to micro- and nanostructured substrates. *J Biomed Mater Res A*. 2004;71:369–376.
25. Pot SA, Liliensiek SJ, Myrna KE, et al. Nanoscale topography–induced modulation of fundamental cell behaviors of rabbit corneal keratocytes, fibroblasts, and myofibroblasts. *Invest Ophthalmol Vis Sci*. 2010;51:1373–1381.
26. Winkler M, Chai D, Kriling S, et al. Nonlinear optical macroscopic assessment of 3-D corneal collagen organization and axial biomechanics. *Invest Ophthalmol Vis Sci*. 2011;52:8818–8827.
27. Lombardo M, Lombardo G, Carbone G, De Santo MP, Barberi R, Serrao S. Biomechanics of the anterior human corneal tissue investigated with atomic force microscopy. *Invest Ophthalmol Vis Sci*. 2012;53:1050–1057.
28. McKee CT, Last JA, Russell P, Murphy CJ. Indentation versus tensile measurements of Young's modulus for soft biological tissues. *Tissue Eng Part B Rev*. 2011;17:155–164.
29. Jester JV, Huang J, Barry-Lane PA, Kao WW, Petroll WM, Cavanagh HD. Transforming growth factor$_{\beta}$–mediated corneal myofibroblast differentiation requires actin and fibronectin assembly. *Invest Ophthalmol Vis Sci*. 1999;40:1959–1967.
30. Jester JV, Huang J, Petroll WM, Cavanagh HD. TGFβ induced myofibroblast differentiation of rabbit keratocytes requires synergistic TGFβ PDGF and integrin signaling. *Exp Eye Res*. 2002;75:645–657.
31. Jester JV, Huang J, Fisher S, et al. Myofibroblast differentiation of normal human keratocytes and hTERT, extended-life human corneal fibroblasts. *Invest Ophthalmol Vis Sci*. 2003;44:1850–1858.
32. Mendonsa R, Myrna KE, Murphy CJ. Substratum compliance modulates TGF-β1–induced myofibroblast transition. In: Abstracts: 49th Annual Meeting of the American Society for Cell Biology, San Diego, California, December 5–9, 2009. *Mol Biol Cell*. 2011b;22:3555 (Abstract 1970/B349).
33. Lakshman N, Petroll WM. Growth factor regulation of corneal keratocyte mechanical phenotypes in 3-D collagen matrices. *Invest Ophthalmol Vis Sci*. 2012;53:1077–1086.
34. Arora PD, Narani N, McCulloch CA. The compliance of collagen gels regulates transforming growth factor-β induction of α-smooth muscle actin in fibroblasts. *Am J Pathol*. 1999;154:871–882.
35. Huang X, Yang N, Fiore VF, et al. Matrix stiffness-induced myofibroblast differentiation is mediated by intrinsic mechanotransduction. *Am J Respir Cell Mol Biol*. 2012;47:340–348.
36. Wang H, Haeger SM, Kloxin AM, Leinwand LA, Anseth KS. Redirecting valvular myofibroblasts into dormant fibroblasts through light-mediated reduction in substrate modulus. *PLoS One*. 2012;7:e39969.
37. Hinz B. Tissue stiffness, latent TGF-β1 activation, and mechanical signal transduction: implications for the pathogenesis and treatment of fibrosis. *Curr Rheumatol Rep*. 2009;11:120–126.
38. Hinz B. Mechanical aspects of lung fibrosis: a spotlight on the myofibroblast. *Proc Am Thorac Soc*. 2012;9:137–147.
39. Liu F, Mih JD, Shea BS, et al. Feedback amplification of fibrosis through matrix stiffening and COX-2 suppression. *J Cell Biol*. 2010;190:693–706.

Investigative Ophthalmology & Visual Science